A&A 452, 811–817 (2006)
DOI: 10.1051/0004-6361:20054617

Astronomy & Astrophysics

The scaling relation of early-type galaxies in clusters

II. Spectroscopic data for galaxies in eight nearby clusters⋆,⋆⋆

D. Bettoni[1], M. Moles[2], P. Kjærgaard[3], G. Fasano[1], and J. Varela[1]

[1] Osservatorio Astronomico di Padova, Vicolo de'll Osservatorio 5, 35122 Padova, Italy
e-mail: [bettoni;fasano;varela]@pd.astro.it
[2] Instituto de Astrofísica de Andalucía, Consejo Superior de Investigaciones Científicas, Camino Bajo de Huétor 50, Apdo. 3004, 18080 Granada, Spain
e-mail: moles@iaa.es
[3] Copenhagen University Observatory, The Niels Bohr Institute for Astronomy, Physics and Geophysics, Juliane Maries Vej 30, 2100 Copenhagen, Denmark
e-mail: per@astro.ku.dk

Received 1 December 2005 / Accepted 22 February 2006

ABSTRACT

Aims. We present low and intermediate resolution spectroscopic data collected for 152 early type galaxies in 8 nearby clusters with $z \leq 0.10$.
Methods. We use low resolution data to produce the redshift and the K-correction for each galaxy, as well as to give their overall spectral energy distribution and some spectral indicators, including the 4000 Å break, the Mg_2 strength and the NaD equivalent width. We have also obtained higher resolution data for early type galaxies in three of the clusters, to determine their central velocity dispersion.
Results. The effect of the resolution on the measured parameters is discussed.
Conclusions. A new accurate systemic redshift and velocity dispersion is presented for four of the surveyed clusters, A98, A3125, A3330, and DC2103-39. We have found that the K-correction values for E/S0 bright galaxies in the given nearby clusters are very similar. We also find that the distribution of the line indicators significantly differs from cluster to cluster.

Key words. galaxies: elliptical and lenticulars, cD – galaxies: distances and redshifts – galaxies: clusters: general

1. Introduction

This is our second paper presenting data on nearby clusters of galaxies. The motivations and details of the program were given in Fasano et al. (2002, hereafter Paper I; see also Fasano et al. 2000), following the proposal discussed by Kjærgaard et al. (1993, hereafter KJM; see also Moles et al. 1998). They will be used together with the results from the project WINGS (Fasano et al. 2006) to analyze the scaling relations of early-type galaxies in clusters.

Here we present low resolution (20 Å and 40 Å, LRS/20 and LRS/40 respectively in the following) and intermediate resolution spectroscopy (3.3 Å resolution, IRS in the following) of 152 early type galaxies in 8 nearby clusters. The LRS data are intended to provide the redshifts of the candidate galaxies, to establish their membership to a given cluster. They also allow the measurement of the K-correction for each individual galaxy and the strength of some spectral features. Rather than the more often used Mg_2, we consider here two other prominent spectral features, the NaD doublet and the 4000 Å break, D4000. The NaD line index is more sensitive to temperature effects than Mg_2, but it can be affected by the presence of interstellar material (Burstein et al. 1984; Bica & Alloin 1986; Bica et al. 1991). However, once allowance is made for that, it correlates well with other indices, Mg_2 in particular. Bica & Alloin (1986) concluded that for a metallicity not greater than solar, any excess of NaD (with respect to the prediction from the Mg_2 indicator) can be due only to interstellar absorption. An outlying position in the Mg_2-NaD plane can therefore be interpreted as a sign of peculiarity (see Bica et al. 1991).

The 4000 Å break, D4000, is primarily sensitive to the presence of young stars. Hamilton (1985) selected it for that reason to study the evolution of early type galaxies with redshift. Dressler & Shectman (1987) concluded that it is not sensitive to metallicity but only to the presence of young stars, and insisted on the adequacy of the break indicator to follow the cosmic evolution of early type galaxies. Kimble et al. (1989) found that D4000 does correlate with some metallicity indicators. The theoretical work by Poggianti & Barbaro (1997) showed that the break is strongly dependent on the effective temperature, and is also sensitive to the metallicity, but only for intermediate temperature stars. On this basis, Barbaro & Poggianti (1997) developed evolutionary models showing that D4000 would be a measure of the present star formation rate. The calibration of D4000 in terms of the atmospheric stellar parameters is rather complicated as many absorption lines are included in the break.

⋆ Based on data obtained with the Nordic Optical Telescope (La Palma, Spain) with ALFOSC. Also based on observations obtained with DFOSC at the D1.54m telescope at the European Southern Observatory (La Silla, Chile).
⋆⋆ Tables 3, 4 and 6 are only available in electronic form at http://www.edpsciences.org

Table 1. Log and setup of the observations.

Run	Date	Mode	Tel.	″/pix	Gr. #	λ range(Å)	Å/pix	Res Å[a]
1	Dec./94	*LR*	*DKT*	0.49	4	3300−6400	3.9	20
2	Sep./95	*LR*	*DKT*	0.49	4	3300−6400	3.9	20
		IR	*DKT*	0.49	13	4800−5800	0.95	3.3
3	Feb./97	*LR*	*NOT*	0.188	7	3800−6800	1.5	20
4	Aug./98	*LR*	*NOT*	0.188	4	3300−6400	3.1	41
5	Aug./99	*LR*	*NOT*	0.188	4	3300−6400	3.1	41
6	Mar./01	*IR*	*NOT*	0.188	13	4800−5800	0.5	1.4

[a] Resolution corresponds to the 2.″5 slit used in all the runs.

Gorgas et al. (1999, and references therein) have made an empirical calibration of the break that can be incorporated into the evolutionary models to predict its value. The most interesting aspect of the break indicator is its sensitivity to recent star formation, and therefore its ability to trace evolution.

The intermediate resolution spectroscopy (IRS) data are necessary to determine the central velocity dispersion needed to build the Fundamental Plane. They also provide more accurate spectral line indices within the covered spectral range. Unfortunately the CCDs we used were very noisy at wavelengths shorter than 5200 Å. Thus the measurement of the Hβ and other indices related to rather weak features was uncertain and we do not include them in the present work.

2. Observations and data reduction

The observations were carried out during several runs from 1994 with the Danish 1.54 m telescope (DKT) at La Silla (Chile), and the Nordic Telescope (NOT) at La Palma (Spain). We used identical focal reducer instruments with both telescopes, DFOSC (DKT) and ALFOSC (NOT), equipped with identical grisms. Some of the data were taken using the MOS possibilities with ALFOSC. The different runs and instrumental setups are given in Table 1. In all observations we used a 2.″5 slit. For the first run the detector was a Thompson 1024 × 1024 CCD with 19 μm pixel, whereas we used various thinned Ford-Loral 2024 × 2024 CCDs with 15 μm pixel for the other runs.

Template stars, for the measure of radial velocities and the velocity dispersion, of spectral type G8-K3 III, were observed each night as well as nearby galaxies with known and accurate data. These were used as a standard to gauge the accuracy of the calibrations. We also observed several flux standard stars to allow the data to be fully calibrated. Identification and positional information for the cluster galaxies are taken from Dressler (1980). Otherwise we measured the positions on the DSS. In Table 3, in Col. 1 we give the name (from NED or Simbad databases), in Cols. 2 and 3 the coordinates and in Col. 4 the reference identification used for the spectrum, this identification is that used in Tables 4 and 6 to identify the galaxies for clusters A98 and A3330. The identifications in Tables 4 and 6 for galaxies in the remaining clusters are from Dressler (1980).

The data reduction procedure was similar for the LRS and IRS data. It was performed within IRAF[1]. The scientific frames were corrected for bias and flat-field and calibrated using a He/Ar arc-lamp. For the MOS data we extracted individual 2D spectra for each object and treated these as any other spectra, so we do not refer to them explicitly in the following.

2.1. The measurement of the redshift. Internal and external accuracy

Before attempting to measure the redshift of the target galaxies, we checked the accuracy of the zero point in the λ-calibration of each spectrum, examining the position of the night sky line [OI]λ5577.32 Å. When necessary the spectrum was shifted to that nominal position. For the radial velocity standard stars, given the short exposure time, the night sky lines were not detected so this procedure could not be applied. We decided to place the standards at zero velocity using their own spectral lines; we then used the IRAF cross-correlation package to control the consistency of the method, i.e., that together, they all define a zero velocity system, within the uncertainties.

The standard stars were then used as templates to measure the redshift of the standard galaxies, using the same IRAF packages. The radial velocity was determined as the mean of the results for the different template stars. The typical scatter is 15 km s^{-1}. In all cases the scatter was within the formal uncertainties of the parameters. The results for those standard galaxies are given in Table 4.

Comparing the results obtained for the standard galaxies from LRS/20 and IRS data (9 cases; there are no galaxies observed in both IRS and LRS/40 modes) we find that the differences in redshift have an average of 7 km s^{-1}, with a scatter of 32 km s^{-1}. Part of that scatter is due to one galaxy, E462G15, for which the IRS result is 71 km s^{-1} higher than the LRS one. Notice that the IRS value is much closer to the redshift reported by Jørgensen et al. (1996, JFK) for that galaxy.

To check the external consistency of the data we have compared them with other sources, JFK (10 galaxies in common, 7 with IRS data) and Smith et al. (2000) (7 objects in common, 5 with IRS data). If we compare only our IRS data, the agreement is excellent with both sources, with σ(diff.) ∼ 15 km s^{-1}. The comparison is also good when LRS data are included, except for EG462G15.

Once the consistency of our measured redshift was assured, we decided to use the standard galaxies as templates to determine the redshift of the target cluster galaxies. We found that they give more accurate results than the standard stars, due to the better spectral matching between both sets of galaxies. Each target object was cross-correlated with all the templates. The average of the resulting z values was taken as the redshift of the galaxy, and the scatter as a quality indicator. The heliocentric redshift values are given in Table 4. The code 1 to 4 corresponds to 1σ values of ≤50 km s^{-1}, between 50 and 100 km s^{-1}, between 100 and 200 km s^{-1}, and between 200 and 300 km s^{-1}. That scatter is typically smaller than 75 km s^{-1}, with more than 75% of values within 150 km s^{-1}, even if it reaches 300 km s^{-1} in some particular cases.

The internal accuracy of the LRS data can be assessed looking at Figs. 1 and 2.

We have searched the literature to examine the external accuracy of our LRS data. The comparison was restricted to those sources for which there are a minimum of 5 galaxies in common. The agreement is in general good as can be seen in Table 2. Our cz values tend to be slightly higher than most of the others. While this cannot be excluded, the differences are about 50 km s^{-1} or

[1] IRAF is the Image Analysis and Reduction Facility made available to the astronomical community by the National Optical Astronomy Observatories, which are operated by the Association of Universities for Research in Astronomy (AURA), Inc., under contract with the US National Science Foundation.

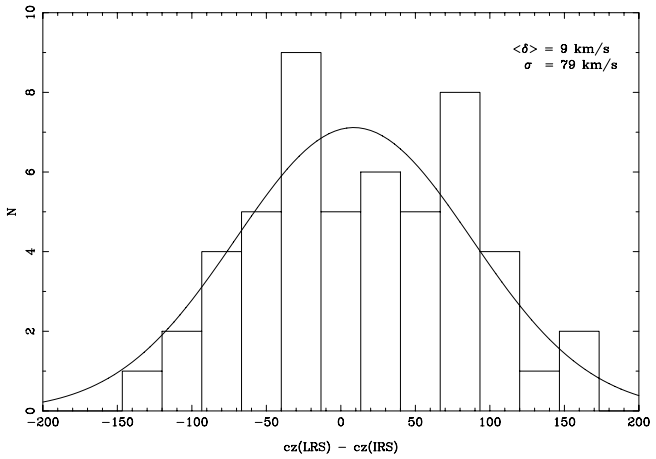

Fig. 1. Distribution of the cz differences for the 52 objects that have both IRS and LRS data. The bin size is 25 km s^{-1}. The solid line is the Gaussian fit to the binned data.

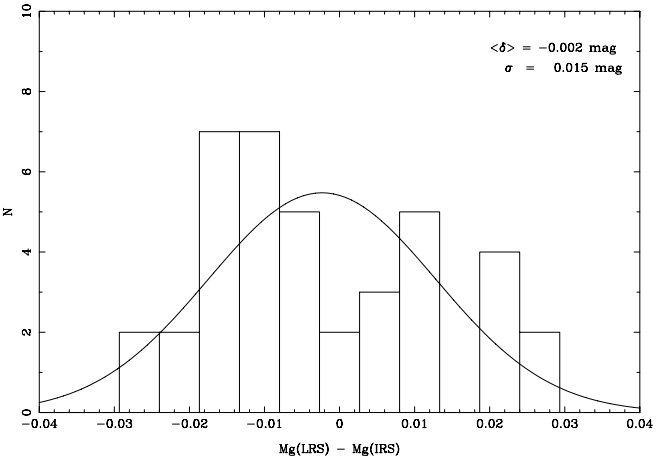

Fig. 2. Distribution of the differences in the Mg_2 values for 42 objects for which both IRS and LRS data are available. The bin size is 0.004. The solid line is the Gaussian fit to the binned data.

less, so we can conclude that our redshift measurements are in the same system as those reported in the quoted references. Indeed, the situation is similar for the IRS data, (see Table 2). The cases for which the disagreement is higher and cannot be accounted for by observational errors have been flagged in Table 4, and commented in the footnotes.

2.2. The measurement of the central velocity dispersion

The velocity dispersion of each target galaxy was determined as the mean of the results for the different template stars. The typical scatter is 10 km s^{-1}. In all cases the scatter was within the formal uncertainties of the parameters. The velocity dispersion and the radial velocity were derived both for the comparison galaxies and for the target galaxies with the Fourier Quotient Technique (Sargent et al. 1977; Bertola et al. 1984), using the standard stars as templates. The results are presented in Table 4. Comparison with the JFK values shows a good agreement. The differences have an rms value of 15 km s^{-1}. Unfortunately the external check can only be done for a handful of target galaxies. We have found independent determinations for only 5 of the galaxies in our sample, all from Wegner et al. (1999). For them, the agreement is also satisfactory since the rms of the differences is the same as for the standard galaxies, 15 km s^{-1}.

Table 2. External comparison of the redshift data.

Cluster		LRS			IRS		
	Ref.	N	$\Delta(cz)$	σ	N	$\Delta(cz)$	σ
*A*98	1	10	+36	147	–	–	–
	2	11	–10	120	–	–	–
*A*119	3	14	+52	75	11	80	48
	4	6	+32	91	6	46	57
	5	5	+3	56	5	28	52
*A*3125	8	6	–11	121	5	–17	133
*A*1069	3	7	+29	116	–	–	–
	6	6	+15	162	–	–	–
*A*1983	7	14	+31	77	–	–	–
*A*2151	7	9	–15	153	–	–	–

References. 1, Beers et al. (1982); 2, Zabludoff et al. (1990); 3, Katgert et al. (1998); 4, Wegner et al. (1999); 5, Huchra et al. (1999); 6, Beers et al. (1991); 7, Dressler & Shectman (1988); 8, Caldwell & Rose (1997).

2.3. The measurement of the K-effect and of the spectral features

To measure the spectral characteristics, the spectra were first shifted to zero redshift, using the measured cz values with the appropriate tasks within IRAF. Then, the K-effect was measured by computing the magnitude in a given band in both the observed and the zero-redshifted spectra. Given the spectral coverage of our data and the redshift of the sources, it was not always possible to compute the K-effect for the three B, V and Gunn r bands. The only band for which we have measured the K-effect for all the targets is V. The results are given in Table 4.

In Table 5 we present the average values for each cluster we have observed. Comparing with the values reported by Pence (1976) for E/S0 galaxies, and with the model predictions by Poggianti (1997) for the same type of galaxies, we find a very good agreement. We notice that the scatter of the K-corrections for early type galaxies in clusters is very small, indicating that applying the same correction to all the bright E/S0 galaxies in clusters introduces only small errors.

To measure the 4000 Å break we chose to use bands of 100 Å width on both sides of the feature. This choice is practical, due to the fact that our spectra do not extend enough into the blue. The data are also collected in Table 4. Even if we cannot directly compare with similar measurements from other authors, we have verified that the range of our values is similar to that found by Dressler & Shectman (1988) for similar galaxies in nearby clusters. For the different line indicators we have used the Lick spectral bands as defined in Worthy et al. (1994). For reasons we have already indicated, only the most prominent features, Mg_2, NaD, and the 4000 Å break were measured. The results are presented in Table 4.

Considering the Mg_2 strength measurements the internal accuracy can be ascertained from repeated measurements with the same resolution. The rms of the differences for galaxies observed twice in the LRS/20 mode is 0.014, most probably due to the poor S/N of some of the spectra we repeated. Thus, as for the redshift, we consider that the overall quality of the data is definitely better than that figure. For the standard galaxies we find a good agreement with JFK values, even if the resolution used is not the same. We notice that the same aperture was used by JFK and here. Except for N1403, for which the Mg_2 value was quoted as uncertain by JFK, as is our own value, due to a rather

Table 5. Average values for the clusters.

Cluster	cz	σ	Mg_2	NaD	D4000	k_B	k_V	k_r
A98	31225	895	0.182–0.346 (0.280)	3.1–6.4 (4.0)	1.45–2.34 (1.95)	0.52 (0.06)	–	–
A119	13260	773	0.195–0.348 (0.303)	2.7–5.3 (4.1)	1.03–2.06 (1.84)	0.22 (0.03)	0.07 (0.02)	0.03 (0.01)
A3125	17898	779	0.208–0.358 (0.294)	2.3–5.0 (3.5)	1.12–2.39 (1.64)	–	0.13 (0.01)	0.09 (0.01)
A3330	27000	695	0.267–0.365 (0.299)	2.1–6.0 (4.0)	1.09–2.75 (1.63)	–	0.14 (0.03)	–
A1069[a]	19671	659	0.175–0.354 (0.269)	2.0–5.5 (3.9)	1.06–2.50 (1.44)	–	0.10 (0.01)	0.07 (0.01)
A1983	13080	948	0.182–0.334 (0.309)	2.5–5.5 (4.5)	1.49–2.39 (1.99)	–	0.07 (0.01)	–
A2151	10980	716	0.264–0.415 (0.320)	2.7–6.0 (4.1)	1.91–2.44 (2.06)	0.19 (0.01)	0.06 (0.01)	–
DC2103	15268	449	0.220–0.338 (0.282)	1.3–4.5 (3.7)	1.11–1.70 (1.37)	0.22 (0.02)	0.09 (0.02)	0.04 (0.01)

The values of cz and σ for A98, A3125, A3330, and DC2103 are from the present work. For the other clusters they have been taken from Struble & Rood (1999).
For the spectral line indicators we give the range and the median value (in parenthesis). For the K-correction only the median value is given.

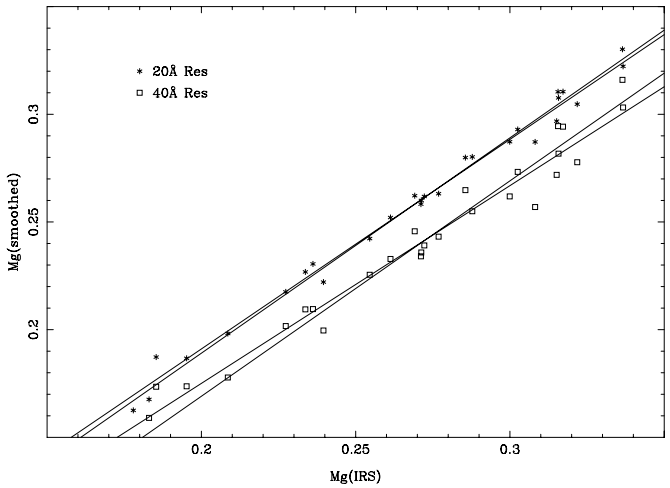

Fig. 3. The relation between the Mg_2 strength values obtained from different resolution data. The plotted lines for the two sets of data are the best fit and the fit with slope =1 in each case.

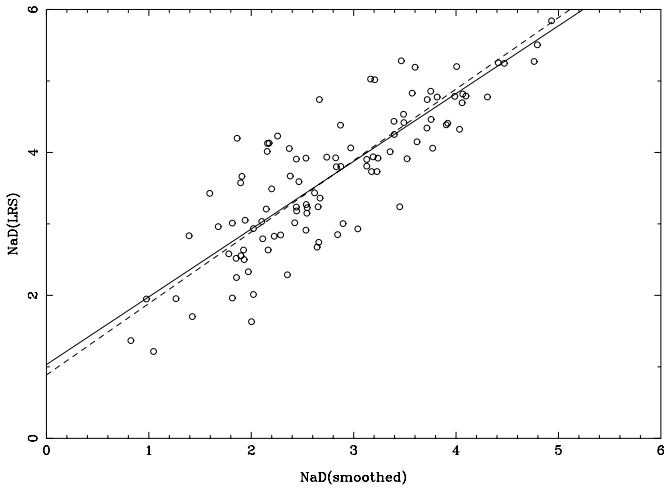

Fig. 4. The EW of the NaD line from real LRS/20 data and from the same spectra degraded to 40 Å resolution. The lines are the best fit and the fit with slope =1.

poor S/N, the rms value of the differences is slightly smaller than 0.01 mag, i.e., smaller than for repeated measurements. As we will discuss below, this difference mainly reflects the effect of the resolution. We notice that the comparison shows that our results are in the same system as those reported by JFK.

The effect of the resolution on the measured values can be checked comparing the results from LRS/40, LRS/20 and IRS data. Starting with the standard galaxies, for the 8 objects measured in LRS/20 and IRS modes, the average difference is 0.004 mag, with an rms value of 0.014 mag. Much of that scatter is due to a single object, N1395, for which the LRS value is 0.028 mag smaller than the IRS value. Regarding the target galaxies, we have 42 objects for which we could measure the Mg2 strength from LRS and IRS data. Excluding three grossly discrepant cases (more than 0.03 mag difference), the differences have an average of 0.003 mag, with σ = 0.014 mag. Their median value is 0.006 mag (see Fig. 2).

To further test the effect, we have degraded the observed IRS data to produce spectra with the resolution of the LRS/20 and LRS/40 modes. The results are presented in Fig. 3. The relations have slopes very close to 1, in particular between LRS/20 and IRS data. The systematic effect can be represented by the relation $Mg_2(IRS) = Mg_2(LRS/20) + 0.011$ mag, with a scatter of 0.004 mag. For the LRS/40 data the correction is 0.031 mag, with a scatter of 0.007 mag.

For the other line indicators, we estimate that the errors are of the order of 5% at worst, a figure that is confirmed by the comparison of the values obtained from repeated measurements. The 4000 Å break is a very robust indicator that is not affected by other aspects, whereas an important resolution effect is expected on the NaD values since the Lick bands used to define the index are rather narrow. Given that the wavelength range of the IRS data does not cover the NaD region, and we do not have enough data taken in both LRS modes for a sound comparison we have simply measured the NaD equivalent width for the LRS/20 data degraded to the resolution of the runs 4 and 5, namely 40 Å. The results are plotted in Fig. 4. We find that the correction is of the form $EW(LRS/20) = EW(LRS/40) + 0.9$ Å. This is the correction we will apply to put all the NaD EW values in the same LRS/20 system.

2.4. Aperture corrections: the final data

To perform the aperture correction of the Mg_2 index we have followed JFK to transform the observed values to the standard aperture of $1.19\,h^{-1}$ kpc, corresponding to 3.″4 at the distance of Coma. Their expression (4) was used to evaluate the correction. As we have already noticed, our data are in a system similar to that of JFK, so we have still to transform our values to put them on the Lick system. This has been done also following JFK,

adding 0.011 to our values. Finally, we have not corrected for the velocity dispersion simply because it is not known for most of our galaxies; for a correction such as that proposed by JFK, it would never be greater than 0.003.

Similarly, aperture corrections should be applied to the other line indicators. For the NaD equivalent width, given that there are no specific data on its radial gradient, we decided to apply the same kind of correction as for the Mg_2 index. The final expression for the aperture corrected NaD line *EW* is given by

$$(EW)_n = W\left[1 - (r_o/r_n)^{-0.016}\right] + (EW)_o \times (r_o/r_n)^{-0.016}$$

where the index n(o) stands for aperture corrected (observed) value, and W is the width of the filter used to measure the feature (32.5 Å in the system defined by Worthy et al. 1994). The maximum correction, for A98, is 0.60 Å, whereas it is of 0.18 Å for A119.

For the aperture correction of the 4000 Å break we have used the result by Sánchez-Blázquez et al. (2001), who have found that the break changes as $-0.20 \log(r)$. The maximum correction is 0.11.

The final, corrected values for the redshift, the velocity dispersion and the line indicators are given in Table 6. We have taken the Mg_2 results from the IRS mode when available, correcting the values obtained with LRS data to that resolution following the methods discussed before, including the correction to place them in the Lick system. For the NaD *EW* value, we have corrected all the LRS/40 measurements to LRS/20 by adding 0.90 Å to take into account the resolution effect as discussed before.

3. General considerations

3.1. The redshift of the clusters

For four clusters, namely A119, A1069, A1983 and A2151, the number of new (or significantly modified) redshift values we can add represents only a small fraction of the total known. There are some cases however, namely A98, A3125, A3330, and DC2103 where that number is significantly increased. Therefore, a new and more precise determination of their redshift and velocity dispersion is possible. We discuss them briefly below. The results are given in Table 5.

We have obtained the redshift for 31 galaxies in the field of A98 (see Table 5), of which 16 are also in Beers et al. (1982), or in Zabludoff et al. (1990), or in both. Following the preceding discussion on the redshift accuracy of our data, we have adopted our values in all cases when they were also given in other references. The redshift distribution of all the galaxies with known cz in the field of A98 is presented in Fig. 5. Considering the 36 objects with cz in the range between 29 500 km s^{-1} and 33 000 km s^{-1}, we find for the cluster redshift $cz = 31\,225$ km s^{-1}, with $\sigma = 895$ km s^{-1}. We notice that 6 of the 7 foreground galaxies define a group with $cz = 17\,973$ km s^{-1}, and $\sigma = 254$ km s^{-1}.

Beers et al. (1982) argued that A98 would comprise two spatially and dynamically distinct extensions. With the new data, a total of 11 galaxies are located in the A98N extension, and 25 in A98S. The velocity distribution shown in Fig. 5 shows only one peak and is rather smooth. There is a slight redshift difference between the northern and southern extensions, but is not significant. Therefore, the existence of two substructures in cz space is not confirmed with the still scarce data available.

Considering A3125, Caldwell & Rose (1997) have reported the redshift of 16 galaxies in the field of the cluster. Only five are also in our sample. Together with our measurements, the total amounts now to 31 values. The cz distribution is given in Fig. 5. Taking out the 5 outliers (2 fore- and 3 background galaxies), we are left with 26 objects, which define the cluster redshift $cz = 17\,898$ km s^{-1}, with $\sigma = 779$ km s^{-1}.

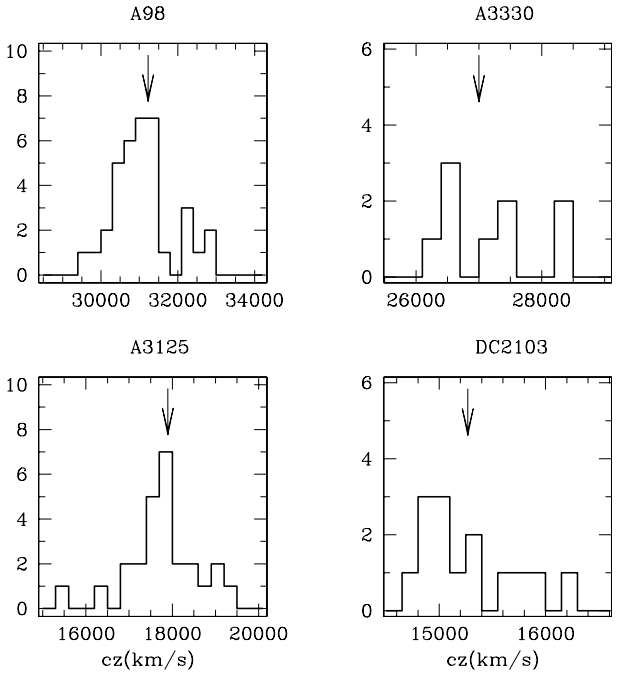

Fig. 5. Distribution of known redshift of galaxies in the clusters A3125, DC2103, A3330 and A98. The arrows indicate the cluster mean cz value as given in the text.

The redshift quoted for A3330 in the compilation by Struble & Rood (1999), $z = 0.0921$, was determined with only two galaxies (Ebeling & Maddox 1997). From the 9 galaxies we have measured, we find $cz = 27\,000$ km s^{-1}, and $\sigma = 695$ km s^{-1}, with the distribution plotted in Fig. 5.

The situation is similar for the cluster DC2103-39, for which only 3 redshifts were known (Loveday et al. 1996). We have measured the redshift of 21 galaxies in the area, of which 6 are foreground and 1 is a background object. For the remaining 14 objects (see Fig. 5) we find $cz = 15\,268$ km s^{-1}, with $\sigma = 449$ km s^{-1}. All the six foreground objects are at a similar redshift. Five of them are grouped with an average $cz = 9260$ km s^{-1}, with $\sigma = 70$ km s^{-1}. These galaxies are located in the field we called "a" in Paper I. They could be part of a cluster as more galaxies are visible in that field.

3.2. The range of spectral properties

In Table 5 we also give the range and median values of the K-correction terms and the spectral indicators we have considered here. The K-correction values, as indicated before, are very similar for all the bright E and S0 galaxies in a given cluster. The average values are very well defined, with a small scatter, and follow the trend with z shown by the data presented by Pence (1976) and with the model prediction by Poggianti (1997) for the same kind of galaxies.

The Mg_2 values span a rather large range in all the 8 clusters (see Fig. 6), in most cases from 0.20 to 0.35. The exceptions are A2151 and A3330 with higher minimum values, what could be due to the small number of objects observed in these clusters. The median values are however different, from

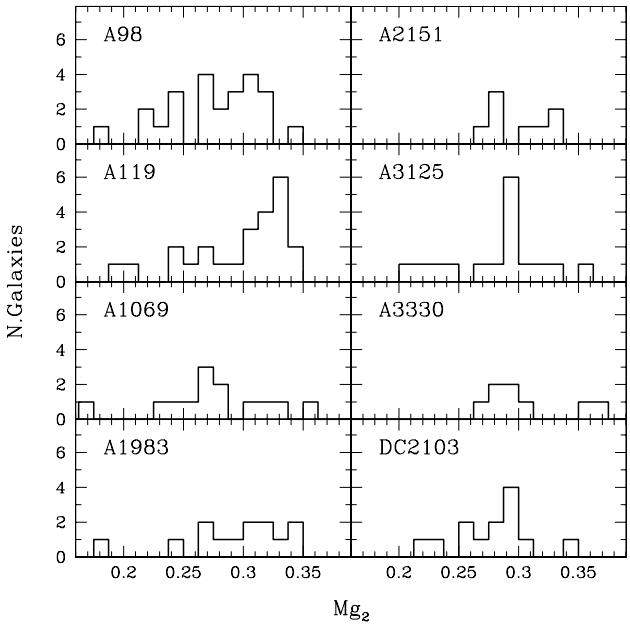

Fig. 6. Distribution of the Mg_2 strength for all the measured galaxies in each cluster.

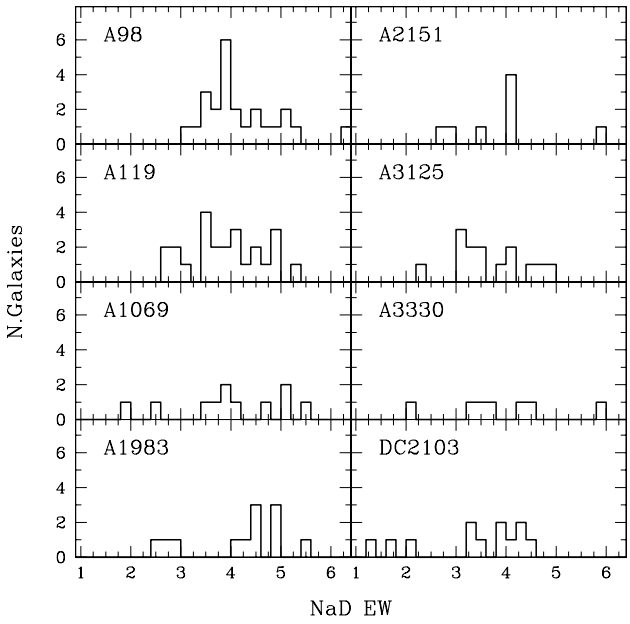

Fig. 7. Distribution of the NaD equivalent width for all the measured galaxies in each cluster.

0.269 mag in A1069 to 0.320 mag in A2151. There is no significant trend with *cz*, finding clusters at similar *cz* with different median values. The situation is similar for the NaD (Fig. 7) equivalent width, which also spans a large range of values in each cluster. The median values are however within 1 Å. Finally, for the 4000 Å break (Fig. 8), there are differences in the ranges, but could be simply due to the small number of sources. We point out the absence of low D4000 values in A2151, and that of high values in DC2103. We notice that a trend is visible between the NaD and Mg_2 indicator, but with an important scatter (see Fig. 9).

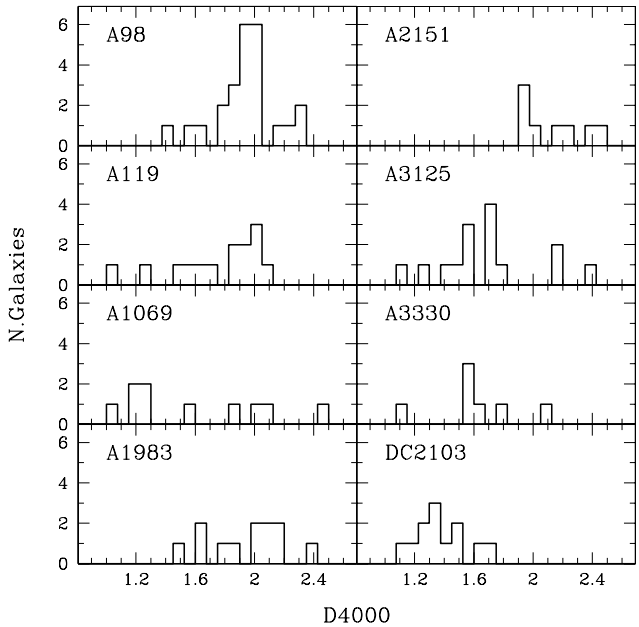

Fig. 8. Distribution of the the 4000 Å break line indicator for all the measured galaxies in each cluster.

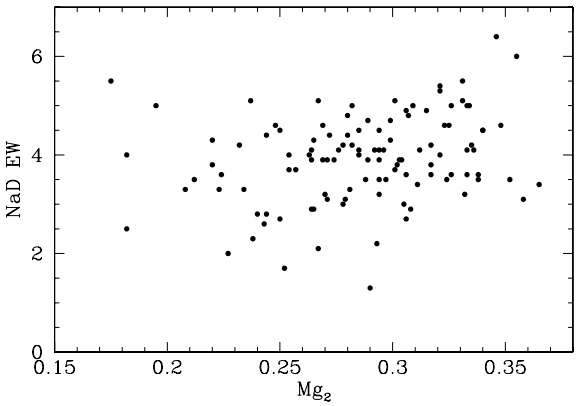

Fig. 9. The Mg_2 strength *versus* the NaD equivalent length for the galaxies in different clusters.

3.3. Galaxies with emission lines

The targets we selected were among the brightest cluster galaxies classified as E or S0, so we did not expect to find many showing emission lines. Out of a total of 13 of such objects objects, half are actually foreground objects relative to the cluster under consideration. These are A1069d41, A3125d11, A3125d14, A98F3g4, and DC2103D18. They all have typical HII-like spectra.

The cluster member galaxies with emission lines are the following:

- A119d44. Faint [OIII]λ5007 detected only in the IRS data.
- A119d45. This galaxy presents a spectrum typical of a star forming region.
- A3125d160.Faint [OIII]λ5007 detected only in the IRS data.
- A3125d77. It presents strong Hα emission, with some structure. There is some indication of high electronic density from the [SII] lines. Neither the [OIII] lines, nor Hβ are visible in our spectrum.
- A2151d78. This galaxy (IC 1182) is a known peculiar early type object, with a spectrum in the border line between star

forming and active galaxies. Its properties have been discussed in Moles et al. (2004).
- A98F1g44. It presents all the lines typical of star forming galaxies, from [OII] to [SII].
- A98F1g58. Spectrum typical of an early type galaxy, but with Hα, [NII] and [SII] clearly visible.
- DC2103d18. Faint [OIII]λ5007 detected only in the IRS data.

We notice that all have spectra of star forming regions, and none shows signs of nuclear activity.

4. Summary and conclusions

We present here LRS and/or IRS for 152 early type galaxies in 8 nearby clusters with $z \leq 0.1$. Data on the redshift, velocity dispersion (for a sub sample), the K-correction, and the most prominent spectral indicators are given.

Comparison of LRS results with IRS and literature data indicate that low resolution spectra can provide accurate values for the redshift (within 65 km s^{-1}), and for the Mg_2 strength (within 0.01 mag). Moreover, since the high and moderate resolution measurements are tightly related, a well defined correction can be applied to obtain all the data in a common base. This means that accurate enough data can be obtained with moderate resolutions, and therefore for galaxies to rather high redshift, an important point for any evolutionary study.

Our data have allowed us to give more precise values for the redshift and velocity dispersion of 4 clusters, poorly known to date, namely A98, A3125, A3330, and DC2103 (see Table 5).

Regarding the K-correction terms, our results indicate that it is very similar for all the bright E/S0 galaxies in a given cluster, so the same correction can be applied to all for many studies. Our values are in very good agreement with the data by Pence (1977) and with the model predictions by Poggianti (1997).

Given the short range in redshift of the clusters analyzed here, no trend with z was expected for any of the spectral indicators, as it is found. It is interesting to note, however, that for all three spectral indicators we find a large range of values for each cluster. It is that physical variance in the spectral properties of the member galaxies that seems to be the most interesting aspect for the present analysis. A trend between the line indicators NaD and Mg_2 is present in our data, in agreement with previous results. The 4000 Å break does not seem to have a clear relation with the other indicators.

References

Barbaro, G., & Poggianti, B. 1997, A&A, 324, 490
Beers, T. C., Geller, M. J., & Huchra, J. P. 1982, ApJ, 257, 23
Beers, T. C., Gebhardt, K., Forman, W., Huchra, J. P., & Jones, C. 1991, AJ, 102, 1581
Bertola, F., Bettoni, D., Rusconi, L., & Sedmak, G. 1984, AJ, 89, 356
Bica, E. L. D., & Alloin, D. 1986, A&A, 166, 83
Bica, E. L. D., Pastoriza, M., Maia, M., da Silva, L., & Dottori, H. 1991, AJ, 102, 1072
Bureau, M., Mould, J. R., & Staveley-Smith, L. 1996, ApJ, 463, 60
Burstein, D., Faber, S. M., Gaskell, C. M., & Krumm, N. 1984, ApJ, 287, 586
Caldwell, N., & Rose, J. A. 1997, AJ, 113, 492
da Costa, L. N., Pellegrini, P. S., Davis, M., et al. 1991, ApJS, 75, 935
Davoust, E., & Considere, S. 1995, A&AS, 110, 19D
van Dokkum, P. G., & Franx, M. 1996, MNRAS, 281, 985
Dressler, A. 1980, ApJS, 42, 565
Dressler, A., & Shectman, S. A. 1987, AJ, 94, 899
Dressler, A., & Shectman, S. A. 1988, AJ, 95, 284
Ebeling, H., & Maddox, S. J. 1995, MNRAS, 275, 1155
Falco, E. E., Kurtz, M. J., Geller, M. J., et al. 1999, PASP, 111, 438
Fasano, G., Poggianti, B. M., Couch, W. J., et al. 2000, ApJ, 542, 673
Fasano, G., Bettoni, D., D'Onofrio, M., Kjærgaard, P., & Moles, M. 2002, A&A, 387, 26 (Paper I)
Fasano, G., Marmo, C., Varela, J., et al. 2006, A&A, 445, 805
Fouqué, P., Gourgoulhon, E., Chamaraux, P., & Paturel, G. 1992, A&AS, 93, 211
Gorgas, J., Cardiel, N., Pedraz, S., & González, J. J. 1999, A&AS, 139, 29
Graham, A. W., Colless, M. M., Busarello, G., Zaggia, S., & Longo, G. 1998, A&AS, 133, 325
Hamilton, D. 1985, ApJ, 297, 371
Huchra, J. P., Vogeley, M. S., & Geller, M. J. 1999, ApJS, 121, 287
Jørgensen, I., Franx, M., & Kjærgaard, P. 1996, MNRAS, 280, 167 (JFK)
Katgert, P., Mazure, A., Perea, J., et al. 1996, A&A, 310, 8
Katgert, P., Mazure, A., den Hartog, R., et al. 1998, A&AS, 129, 399
Kimble, R. A., Davidsen, A. F., & Sandage, A. R. 1989, ApJS, 157, 237
Kjærgaard, P., Jørgensen, I., & Moles, M. 1993, ApJ, 418, 617 (KJM)
Lauberts, A., & Valentjin, E. A. 1989, The Surface Photometry Catalogue of the ESO-Uppsala Galaxies, Garching bei München, ESO
Loveday, J., Efstathiou, G., Maddox, S. J., & Peterson, B. A. 1996, ApJ, 468, 1
Moles, M., Campos, A., Kjaegaard, P., Fasano, G., & Bettoni, D. 1998, ApJ, 495, L31
Moles, M., Bettoni, D., Fasano, G., Kjaegaard, P., Varela, J., & Milvang-Jensen, B. 2004, A&A, 418, 495
Paturel, G., Petit, C., Prugniel, P., et al. 2003, A&A, 412, 45
Pence, W. 1976, ApJ, 203, 39
Poggianti, B. M., & Barbaro, G. 1997, A&A, 325, 1025
Poggianti, B. M. 1997, A&AS, 122, 399
Postman, M., & Lauer, T. R. 1995, ApJ, 440, 28
Sánchez-Blázquez, P., Gorgas, J., Cardiel, N., et al. 2001, Ap&SS, 277, 351
Sargent, W. L. W., Schechter, P. L., Boksenberg, A., & Shortridge, K. 1977, ApJ, 212, 326
Simien, F., & Prugniel, P. 1997, A&AS, 126, 519
Smith, R. J., Lucey, J. R., Hudson, M. J., Schlegel, D. J., & Davies, R. L. 2000, MNRAS, 313, 469
Struble, M. F., & Rood, H. J. 1999, ApJS, 125, 35
de Vaucouleurs, G., de Vaucouleurs, A., Corwin, Jr., H. G., et al. 1991, Third Reference Catalogue of Bright Galaxies, RC3
Wegner, G., Colless, M., Saglia, R. P., et al. 1999, MNRAS, 305, 259
Worthy, G., Faber, S. M., González, J., & Burstein, D. 1994, ApJS, 94, 687
Zabludoff, A. I., Huchra, J. P., & Geller, M. J. 1990, ApJS, 74, 1
Zabludoff, A. I., Geller, M. J., Huchra, J. P., Vogeley, M. S. 1993, AJ, 106, 1273

Online Material

Table 3. Galaxies not included in Dressler (1980).

Galaxy	α(2000)	δ(2000)	*Spectrum id.*
Abell 98			
$2MASXJ00463567+2029428$	00 : 46 : 35.7	+20 : 29 : 42	$F1g20$
$2MASXJ00463524+2030108$	00 : 46 : 35.3	+20 : 30 : 11	$F1g22$
$A98:[BGH82]320$	00 : 46 : 24.7	+20 : 30 : 07	$F1g30$
$2MASXJ00462380+2030006$	00 : 46 : 23.9	+20 : 30 : 00	$F1g31$
$2MASXJ00462059+2029076$	00 : 46 : 20.7	+20 : 29 : 07	$F1g38$
$2MASXJ00461931+2029416$	00 : 46 : 19.4	+20 : 29 : 41	$F1g43$
$A98:[BGH82]311$	00 : 46 : 16.0	+20 : 30 : 19	$F1g44$
$2MASXJ00463702+2026068$	00 : 46 : 37.1	+20 : 26 : 06	$F1g58$
$2MASXJ00462586+2027326$	00 : 46 : 25.9	+20 : 27 : 32	$F1g65$
$3C021$	00 : 46 : 29.4	+20 : 28 : 04	$F1g76$
$2MASXJ00463318+2027518$	00 : 46 : 33.2	+20 : 27 : 51	$F1g77$
$2MASXJ00463183+2028118$	00 : 46 : 31.9	+20 : 28 : 11	$F1g80$
$2MASXJ00463624+2028268$	00 : 46 : 36.3	+20 : 28 : 26	$F1g88$
$2MASXJ00463624+2028268$	00 : 46 : 08.5	+20 : 28 : 50	$F2g01$
$2MASXJ00460743+2028486$	00 : 46 : 07.5	+20 : 28 : 48	$F2g02$
$A98:[PBL2000]0264$	00 : 46 : 04.8	+20 : 28 : 27	$F2g03$
$2MASXJ00455043+2027487$	00 : 45 : 50.5	+20 : 27 : 49	$F2g05$
$2MASXJ00455043+2027487$	00 : 45 : 50.4	+20 : 29 : 08	$F2g07A$
$2MASXJ00455008+2029097$	00 : 45 : 50.2	+20 : 29 : 09	$F2g07B$
$2MASXJ00460209+2030516$	00 : 46 : 02.2	+20 : 30 : 50	$F2g09$
$2MASXJ00461355+2034516$	00 : 46 : 13.6	+20 : 34 : 51	$F3g01$
$2MASXJ00460400+2034516$	00 : 46 : 04.0	+20 : 34 : 51	$F3g02$
$A98:[BGH82]182$	00 : 45 : 59.8	+20 : 35 : 09	$F3g03$
$NPM1G+20.0024$	00 : 45 : 52.9	+20 : 35 : 13	$F3g04$
$A98:[PBL2000]376$	00 : 45 : 57.5	+20 : 36 : 56	$F3g05$
$2MASXJ00460400+2034516$	00 : 46 : 04.5	+20 : 36 : 45	$F3g07$
$A98:[PBL2000]269$	00 : 46 : 17.1	+20 : 23 : 44	$F10g5$
$2MASXJ00461469+2023426$	00 : 46 : 14.7	+20 : 23 : 42	$F10g6$
$2MASXJ00462849+2023488$	00 : 46 : 28.5	+20 : 23 : 48	$F10g7$
$2MASXJ00463390+2023548$	00 : 46 : 34.0	+20 : 23 : 55	$F10g8$
$2MASXJ00463852+2022538$	00 : 46 : 38.6	+20 : 22 : 53	$F10g9$
Abell 3330			
$2MASXJ05145263-4859071$	05 : 14 : 52.5	-48 : 59 : 07	$g21$
$2MASXJ05145588-4859121$	05 : 14 : 55.7	-48 : 59 : 12	$g22$
$2MASXJ05150675-4901321$	05 : 15 : 06.6	-49 : 01 : 33	$g5$
$2MASXJ05150726-4902261$	05 : 15 : 07.2	-49 : 02 : 27	$g6$
$APMUKS(BJ)B051342.65-490606.2$	05 : 15 : 00.7	-49 : 02 : 48	$g7$
$FAIRALL0790$	05 : 14 : 39.4	-49 : 03 : 29	$g1$
$2MASXJ05143494-4905153$	05 : 14 : 34.9	-49 : 05 : 15	$g2$
$2MASXJ05150574-4905461$	05 : 15 : 05.6	-49 : 05 : 47	$g4$
$2MASXJ05142945-4905534$	05 : 14 : 29.3	-49 : 05 : 54	$g3$

Table 4. Observed parameters of the standard and cluster galaxies.

Galaxy	LRS data										IRS data					
	cz	Q	Refs.	k_B	k_V	k_r	D4000	Mg_2	NaD	Run	cz	ϵ	σ	ϵ	Mg_2	Comments
Std Gal																
N541	5427	1	a, b	.08	.02	−.03	1.76	.296	3.4	5	–	–	–	–	–	–
N720	1758	1	a, b	.02	.01	.00	–	.318	4.5	2	1729	17	223	74	.323	–
N1395	1699	1	a, b	–	.01	.00	–	.316	4.9	1	1667	38	275	28	.344	–
N1399	1450	1	a, c	–	.01	.00	–	.341	5.3	2	1445	51	364	74	.336	–
N1403	4292	1	a, d	–	.02	.00	1.82	.281	3.2	2	4281	36	178	43	.265	–
N1406	1357	1	e	.02	.01	.00	2.17	.266	2.8	2	–	–	–	–	–	–
N1426	1409	1	a, f	–	.01	.00	–	–	3.9	2	1425	17	156	23	.260	$\Delta V = 172$
N1726	3964	1	a, g	–	–	–	–	.288	4.1	5	–	–	–	–	–	–
N2340	5971	1	b	–	–	–	2.48	.335	5.8	3	5938	37	241	33	.337	–
N2974	–	–	–	–	–	–	–	–	–	4	1980	51	253	35	.289	–
N2986	2336	1	a, b	–	.01	.00	–	.319	5.3	1	–	–	–	–	–	–
E462G15	5751	1	a, h	–	.04	.01	1.87	.292	3.9	2	5812	75	263	15	.272	-
N7507	1538	1	d	–	.01	.01	–	.335	5.0	2	1578	18	206	26	.325	–
N7562	3583	1	b	–	.03	.02	2.47	.294	4.7	2	3606	58	242	17	.288	–
N7619	3804	1	a, b	.05	.03	.02	1.82	.320	4.9	2	3801	41	275	35	.312	–
Abell 98																
F1g20	32 104[a]	4	–	.57	–	–	1.92	.207	1.7	4	–	–	–	–	–	–
F1g22	30 852	3	–	.60	–	–	2.24	.187	3.0	4	–	–	–	–	–	–
F1g30	31 358	2	–	.56	–	–	1.82	.185	3.1	4	–	–	–	–	–	–
F1g31	29 984	2	–	.60	–	–	2.23	.243	2.1	4	–	–	–	–	–	–
F1g38	31 021[b]	2	–	.60	–	–	2.12	.231	2.4	4	–	–	–	–	–	–
F1g43	33 099	3	–	.61	–	–	2.19	.216	1.6	4	–	–	–	–	–	–
F1g44	30 605[c]	2	–	–	–	–	–	–	–	4	–	–	–	–	–	EL
F1g58	30 654	1	–	–	–	–	–	–	–	5	–	–	–	–	–	EL
F1g65	31 049	2	–	.62	–	–	2.08	.258	2.5	4	–	–	–	–	–	–
F1g76	30 898	2	–	.57	–	–	1.93	.283	4.9	5	–	–	–	–	–	–
F1g77	42 272[d]	2	–	.55	–	–	1.51	.178	3.0	4	–	–	–	–	–	–
F1g80	32 312	2	–	.57	–	–	1.91	.226	2.4	5	–	–	–	–	–	–
F1g88	32 122	1	–	.61	–	–	1.93	.258	3.9	4, 5	–	–	–	–	–	–
F2g1	30 484	3	–	.40	–	–	1.45	.119	2.5	5	–	–	–	–	–	Hβ abs.
F2g1A	31 475	2	–	.51	–	–	1.92	.201	2.6	5	–	–	–	–	–	–
F2g3	31 605	2	–	.52	–	–	1.83	.181	2.9	5	–	–	–	–	–	–
F2g5	31 100	2	–	.51	–	–	1.85	.239	2.3	5	–	–	–	–	–	–
F2g7A	31 005	3	–	.51	–	–	1.85	.243	3.4	5	–	–	–	–	–	–
F2g7B	30 510	1	–	.52	–	–	1.68	.218	1.8	5	–	–	–	–	–	–
F2g9	30 151	3	–	.53	–	–	1.92	.238	3.6	5	–	–	–	–	–	–
F3g1	17 871	1	–	.29	–	–	1.89	.279	2.9	5	–	–	–	–	–	–
F3g2	30 169	2	–	.57	–	–	1.76	.233	2.6	5	–	–	–	–	–	–
F3g3	31 164[e]	2	–	.48	–	–	1.76	.217	3.3	5	–	–	–	–	–	–
F3g4	10 988	1	–	–	–	–	–	–	–	5	–	–	–	–	–	EL
F3g5	30 343	2	–	.41	–	–	1.35	.157	2.3	5	–	–	–	–	–	–
F3g7	31 284	2	–	.49	–	–	1.85	.261	2.0	5	–	–	–	–	–	–
F10g5	35 868	1	–	.55	–	–	1.82	.205	1.7	5	–	–	–	–	–	–
F10g6	31 037	1	–	.52	–	–	1.87	.211	2.4	5	–	–	–	–	–	–
F10g7	30 370	1	–	.49	–	–	1.68	.174	3.6	5	–	–	–	–	–	–
F10g8	32 834	1	–	.52	–	–	1.76	.201	2.4	5	–	–	–	–	–	–
F10g9	31 094	1	–	.45	–	–	1.53	.161	2.1	5	–	–	–	–	–	–
Abell 119																
D26	13 539	1	–	–	.08	.03	1.87	.259	3.8	2	13 462	24	173	66	.246	–
D36	13 958	2	–	.26	.04	.03	1.93	.269	2.7	4	–	–	–	–	–	–
D37	12 959	1	1, 3, 4	–	.08	.03	–	.319	4.8	1	12 872	26	240	30	.309	$\Delta V = 55$
D38	12 591	1	1	.22	.04	–	1.88	.269	2.5	4	–	–	–	–	–	–
D41	12 408	1	1,3	–	.07	.03	–	–	3.9	1	12 342	38	173	22	.316	$\Delta V = 250$
D44[f]	13 184	1	1	–	.06	.02	–	.298	3.0	1	13 081	66	201	35	.315	EL
D45	12 660	1	–	–	–	–	–	–	–	1	–	–	–	–	–	EL
D47	14 521	3	1	.22	.10	.04	1.27	.281	2.8	2	14 628	40	194	37	.261	$\Delta V = 186$
D49	13 810	2	1	–	.09	.05	1.62	.219	2.5	2	13 733	67	291	43	.233	–
D51	12 540	1	1	.24	.03	–	1.96	.273	4.2	4	–	–	–	–	–	–
D52	13 413	1	1, 2, 3, 5	–	.08	.03	1.81	–	4.4	1, 2	13 447	50	264	30	.331	–

Table 4. continued.

Galaxy	LRS data										IRS data					
	cz	Q	Refs.	k_B	k_V	k_r	D4000	Mg_2	NaD	Run	cz	ϵ	σ	ϵ	Mg_2	Comments
D60	11 475	2	1, 2, 3, 6	–	.06	.02	–	.288	4.1	1	11 565	56	331	25	.302	–
D62	12 990	3	1	–	.07	.03	–	.313	3.4	1	13 077	28	161	19	.321	$\Delta V = 70$
D66	13 318	1	1, 2, 3, 6	–	.07	.02	–	.295	4.8	1	13 356	50	270	55	.317	–
D68	12 143	2	1	–	.07	.02	–	.264	4.4	1	12 225	44	220	42	.308	$\Delta V = 380$
D74[g]	12 663	1	1	–	.05	.01	–	.252	3.5	1	12 647	61	249	28	.240	–
D75[h]	11 532	1	1, 5	–	.05	.01	–	.261	2.7	1, 2	11 560	66	167	31	.256	–
D93[i]	11 703	2	1, 5	–	.05	.02	–	.297	4.5	1	11 705	48	210	72	.272	–
D94	12 553	1	1, 5	.23	.04	–	2.03	.264	3.0	4	–	–	–	–	–	–
D99[j]	13 698	2	1	–	.07	.05	–	–	2.8	1, 2	13 540	59	268	34	.288	–
D102	13 230	1	1	–	.07	.04	2.00	.161	4.8	1, 2	13 258	61	196	48	.178	–
D105	13 335	1	1,2,3	–	.08	.03	1.67	–	3.7	1	13 350	62	313	89	.286	–
D107[k]	13 184	2	1	.16	.06	.01	1.00	–	3.4	2	13 085	68	157	35	.316	Δ V = 107
D109[l]	13 029	1	1,5	–	.05	.01	–	.202	3.3	1, 2	13 021	57	224	8	.195	–
D111	12 615	1	–	.20	.08	.04	1.55	.262	4.2	2	12 585	70	249	54	.255	–
D112[m]	14 560	3	1	.19	.06	0.02	1.43	.196	2.6	2	14 650	72	219	45	.227	–
D114[n]	13 312	2	1	–	.07	.03	2.00	.288	3.9	2	13 375	40	128	11	–	$\Delta V = 90$
Abell 3125																
D9	18 508	1	–	–	.14	.08	1.45	.261	–	1	–	–	–	–	–	–
D11	8682[o]	1	1,8	–	.02	.03	–	–	–	1	–	–	–	–	–	EL
D14	15 532	1	–	–	.15	.12	–	–	–	1	–	–	–	–	–	EL
D46	17 900	3	9	–	.13	.08	1.64	.270	4.4	1	17 830	38	253	24	.276	$\Delta V = 50$
D47	17 816	2	9	–	.13	.09	1.76	.241	3.8	1	17 745	31	299	42	.269	–
D48	17 346	1	9	–	.12	.08	2.14	.189	3.0	1	–	–	–	–	–	–
D51	18 790	1	–	–	.14	.09	2.08	.282	4.3	1, 2	18 845	36	213	46	.300	–
D60	17 587	1	9	–	.13	.09	1.54	.255	3.6	1	17 478	45	291	59	.281	–
D77	17 440	2	–	–	.11	.07	–	–	–	1	17 298	70	261	67	–	EL
D88	17 675	2	–	–	.14	.09	1.06	.332	4.7	1	17 693	71	332	85	.310	$\Delta V = 189$
D93	17 485	1	9	–	.11	.07	1.22	.259	2.9	2	17 621	35	287	77	.271	–
D95	–	-	–		–	–	–	–	–	–	17 866	61	335	34	.263	$\Delta V = 73$
D96	17 702	3	9	–	.13	.10	2.33	.198	2.0	1	17 652	48	239	22	.215	–
D103	17 786	1	–	–	.13	–	1.54	.177	3.0	2	17 766	49	288	11	.185	–
D104	18 099	1	–	–	.14	.09	1.67	.237	2.8	1	–	–	–	–	–	–
D129	18 890	1	9	–	.13	.09	1.47	.231	2.6	1	–	–	–	–	–	–
D130	19 112	2	9	–	.13	.09	1.53	.281	3.2	1	19 049	27	236	25	.271	–
D140	18 917	2	9	–	.15	.10	1.64	.211	3.9	1	18 945	39	212	5	.209	–
D160	18 361	1	9	–	.15	.10	1.39	.263	3.2	1	18 459	46	262	61	–	EL
D161	18 115	2	–	–	.14	.10	1.68	.315	2.8	1, 2	17 964	79	328	35	.336	–
Abell 3330																
G1	27 522	2	–	–	.10	–	1.54	.244	4.0	1	–	–	–	–	–	–
G2	26 446	2	–	–	.10	–	1.00	.226	1.6	1	–	–	–	–	–	–
G3	27 358	2	–	–	.15	–	2.66	.260	3.2	1	–	–	–	–	–	–
G4	26 586	3	–	–	.13	–	1.97	.242	–	1	–	–	–	–	–	–
G5	28 262	1	–	–	.17	–	1.45	.314	5.5	1	–	–	–	–	–	–
G6	27 140	1	–	–	.14	–	1.68	.258	3.8	1	–	–	–	–	–	–
G7	26 222	1	–	–	.11	–	–	–	–	1	–	–	–	–	–	EL
G21	26 463	1	–	–	.19	–	1.50	.324	2.9	1	–	–	–	–	–	–
G22	28 251	1	–	–	.20	–	1.44	.247	3.0	1	–	–	–	–	–	–
Abell 1069																
D3	19 336	1	–	–	.10	.07	1.16	.232	4.8	1	–	–	–	–	–	–
D9	19 478	3	–	–	.11	.07	2.44	.234	3.6	1	–	–	–	–	–	–
D12	16 624	2	7	–	.08	.07	1.66	.253	2.3	1	–	–	–	–	–	–
D14	16 656	1	–	–	.08	.07	1.38	.275	3.6	1	–	–	–	–	–	–
D15	19 737	1	1,7	–	.10	.07	1.51	.235	3.9	1, 6	19 709	23	239	9	.292	–
D16	20 110	4	1	–	.09	.07	1.00	.140	5.2	1	–	–	–	–	–	–
D19	18 030	1	1,7	–	.10	.08	1.10	.224	3.7	1, 6	18 040	31	220	11	.261	–
D21	19 817	2	1,7	–	.11	.06	1.20	.319	3.2	1, 6	19 345	31	357	9	.328	–
D25	20 331	1	1,7	–	.09	.04	1.82	.212	2.3	1, 6	20 287	19	275	7	.219	–
D29	20 051	1	1,7	–	.10	.07	2.00	.259	4.5	1, 6	20 067	17	236	7	.283	–
D30	20 430	1	1	–	.08	.06	1.22	.219	3.4	1	–	–	–	–	–	–
D38	19 329	2	–	–	.11	.08	–	.244	–	1, 6	19 432	19	295	7	–	–

Table 4. continued.

Galaxy	LRS data										IRS data					
	cz	Q	Refs.	k_B	k_V	k_r	D4000	Mg_2	NaD	Run	cz	ϵ	σ	ϵ	Mg_2	Comments
D39	19 729	3	–	–	.09	.07	–	.192	1.7	1	–	–	–	–	–	–
D41	11 644	1	–	–	–	–	–	–	–	1	–	–	–	–	–	EL
D46	19 700	2	–	–	.09	.05	1.97	.248	4.8	1, 6	19 653	19	231	8	.307	–
D47	–	-	–	–	–	–	–	–	–	6	18 931	14	149	10	.250	–
Abell 1983																
D6	17 547	1	10	–	–	–	1.66	.186	2.0	3	–	–	–	–	–	–
D10	13 156	1	10	–	.07	–	1.60	.303	5.3	3	–	–	–	–	–	–
D15	13 589	1	10	–	.07	–	2.11	.292	4.3	3, 6	13 676	20	323	7	.323	–
D23	12 782	1	10	–	.05	–	1.46	.154	2.3	3	–	–	–	–	–	–
D24	13 504	1	10	–	.07	–	1.59	.241	4.4	3	–	–	–	–	–	–
D26	17 822	1	10	–	–	–	1.90	.294	4.4	3	–	–	–	–	–	–
D28	6251	1	10	–	.04	–	1.59	.180	2.0	3	–	–	–	–	–	–
D35	13 659	1	10	–	.08	–	2.36	.237	4.1	3	–	–	–	–	–	–
D46	13 532	1	10	–	.07	–	2.15	.280	2.7	3	–	–	–	–	–	–
D54	13 167	2	7	–	.07	–	1.79	.297	4.7	3,6	12 979	14	232	7	.298	–
D56	13 481	1	10	–	.07	–	2.04	.285	4.8	3,6	13 583	20	198	9	.265	–
D58	13 606	1	11	–	.07	–	2.03	.212	2.6	3	–	–	–	–	–	–
D77	–	-	–	–	–	–	–	–	–	6	13 844	15	215	8	.266	–
D78	13 781	1	7	–	.06	–	1.85	.306	3.9	3,6	13 639	15	212	8	.277	–
D84	13 894	1	11	–	.08	–	1.96	.281	4.8	3	–	–	–	–	–	–
D105	13 310	1	10	–	.06	–	1.98	.264	4.3	3,6	13 387	20	323	7	.323	–
Abell 2151																
D4	9986	3	10	.18	.06	–	1.91	.219	1.9	4	–	–	–	–	–	–
D7	10 055	1	2	.20	.07	–	2.23	.290	3.2	4	–	–	–	–	–	–
D9	10 248	1	10	.18	.06	–	1.90	.261	1.7	4	–	–	–	–	–	–
D15	9966	1	10	.19	.06	–	1.96	.281	2.6	4	–	–	–	–	–	–
D40	10 330	1	12	.19	.04	–	2.12	.268	3.1	4,6	10 050	15	230	7	.271	–
D62	9338	1	2	.18	.06	–	2.36	.233	3.2	4	–	–	–	–	–	–
D63	10 830	1	10	.21	.07	–	2.43	.281	3.1	4,6	10 455	16	195	9	.262	–
D64	10 432	2	10	.21	.07	–	1.97	–	5.0	4	–	–	–	–	–	–
D65	–	-	–	–	–	–	–	–	–	6	10 426	13	291	6	.305	–
D66	–	-	–	–	–	–	–	–	–	6	9643	9	186	6	.270	–
D78	10 262	1	–	.13	.05	–	–	–	–	4	–	–	–	–	–	EL
D134	–	-	–	–	–	–	–	–	–	6	11 074	50	318	11	.302	–
DC 2103-39																
D3	16 114	1	–	.26	.13	.03	1.33	.268	4.2	2	16 152	35	185	27	.272	$\Delta V = 150$
D14	9374	1	–	.13	.05	.02	1.28	.329	4.9	2	9343	40	332	58	.327	–
D15	15 034	1	–	.23	.09	.04	1.32	.335	3.2	2	15 038	39	237	30	.316	$\Delta V = 103$
D18	9319	2	–	–	.05	.03	–	–	–	2	9208	30	137	38	–	EL, $\Delta V = 122$
D20	9287	1	–	.11	.04	.02	1.00	.185	1.8	2	9353	19	154	38	.191	–
D21	9161	1	–	.15	.06	.03	1.49	.229	2.5	2	9400	31	242	64	.218	$\Delta V = 91$
D23	9279	1	–	.13	.07	.03	1.25	.273	2.6	2	9245	62	260	52	.244	$\Delta V = 270$
D38	15 820	1	–	.22	.08	.04	1.60	.232	3.0	2	15 742	52	275	47	.212	–
D39	15 869	3	–	.26	.09	.04	1.19	.252	1.0	2	15 892	51	313	23	.268	–
D40	15 060	1	–	.22	.08	.04	1.47	.249	3.9	2	14 992	33	223	17	.260	–
D42	14 719	1	–	.20	.10	–	1.47	.240	3.6	2	14 700	24	206	71	.249	–

Table 4. continued.

Galaxy	LRS data										IRS data					
	cz	Q	Refs.	k_B	k_V	k_r	D4000	Mg_2	NaD	Run	cz	ϵ	σ	ϵ	Mg_2	Comments
D53	26 506	1	–	–	.13	–	1.97	.287	3.7	2	26 558	60	316	23	–	–
D60	15 635	2	–	.22	.11	.05	1.25	.224	3.7	2	15 626	32	177	58	.232	–
D61	15 369	2	–	.20	.10	.04	1.33	.278	3.1	2	15 326	33	200	69	–	–
D62	15 149	1	–	–	.07	.03	1.07	.227	1.4	2	15 079	23	176	17	.230	–
D63	15 003	2	–	–	.08	.03	1.16	–	1.9	2	14 937	23	147	24	.271	–
D66	9527	2	–	–	.04	.02	1.18	.166	0.8	2	9581	39	235	23	.177	–
D71	14 836	1	–	–	.08	.04	1.37	.249	4.1	2	14 832	44	207	33	.258	–
D73	–	-	–	–	–	–	–	–	–	-	14 940	38	260	17	.276	–
D76	15 230	3	–	.20	.08	.03	1.66	.187	4.0	2	–	–	–	–	–	–
D102	–	-	–	–	–	–	–	–	–	-	15 324	39	207	55	–	$\Delta V = 92$

References for the redshift. (A) Standard Galaxies: [a] JFK; [b] Smith et al. (2000); [c] Graham et al. (1998); [d] de Vaucouleurs et al. (1991, RC3); [e] Bureau et al. (1996); [f] Lauberts & Valentijn (1989, ESO-Uppsala Catalog); [g] Simien and Prugniel (1997); [h]: da Costa et al. (1991). (B) Cluster Galaxies. 1: Katgert et al. (1998, ENACS Catalog); 2, de Vaucouleurs et al. (1991, RC3); 3, Huchra et al. (1999, CfA Catalog); 4, Zabludoff et al. (1993); 5, Paturel et al. (2003, LEDA Catalogue); 6, Postman & Lauer (1995); 7, Beers et al. (1991); 8, Lauberts & Valentijn (1989, ESO-Uppsala Catalog); 9, Caldwell & Rose (1997); 10, Dressler & Shectman (1988); 11, Zabludoff et al. (1990); 12, Davoust & Considere (1995).

Notes on discrepant redshift results:

- [a] In agreement with B82, but 394 km s^{-1} higher than in Zabludoff et al. (1990).
- [b] 634 km s^{-1} higher than in Z90.
- [c] Our value, determined form the emission lines, agrees with Z90, but it is 735 km s^{-1} lower than in Beers et al. (1982).
- [d] Our value agrees with Z90, and is 9826 km s^{-1} higher than in Beers et al. (1982).
- [e] The redshift we find for this galaxy is 368 km s^{-1} higher than in Beers et al. (1982), but grossly discrepant with Zabludoff et al.(1990).
- [f] Observed in LRS and IRS modes with concordant results. Our LRS value is 337 km s^{-1} higher than in the ENACS Catalogue.
- [g] Observed in LRS and IRS modes with concordant results. Our LRS value is 1038 km s^{-1} lower than in the ENACS Catalogue, and very close to that reported by Fouqué et al. (1992).
- [h] Observed twice in LRS mode and in IRS mode, with concordant results. Our LRS value is 1330 km s^{-1} lower than in the ENACS Catalogue.
- [i] Observed in LRS and IRS modes with concordant results. Our LRS value is 1357 km s^{-1} lower than in the ENACS Catalogue. The redshift reported by Falco et al. (1999) is very close to our value, whereas that reported by Fouqué et al. (1992) does not agree with any of previous determinations.
- [j] Observed in LRS and IRS modes with concordant results. Our LRS value is 1226 km s^{-1} higher than in the ENACS Catalogue.
- [k] Observed in LRS and IRS modes with concordant results. Our LRS value is 1210 km s^{-1} lower than in the ENACS Catalogue. The redshift reported by Fouqué et al. (1992) is very close to our value.
- [l] Observed in LRS and IRS modes with concordant results. Our LRS value is 2086 km s^{-1} higher than in the ENACS Catalogue.
- [m] Observed in LRS and IRS modes with concordant results. Our LRS value is 2819 km s^{-1} higher than in the ENACS Catalogue.
- [n] Observed in LRS and IRS modes with concordant results. Our LRS value is 5393 km s^{-1} lower than in the ENACS Catalogue.
- [o] Our redshift is 9478 km s^{-1} lower than in the ENACS Catalogue, that is in agreement with the redshift given in the ESO-Uppsala catalog. Our value is from the detected emission lines.

Table 6. The adopted, fully corrected, redshift and spectral indicators.

Galaxy	cz	D4000	NaD	Mg_2	$\log\sigma$
Abell 98					
F1g20	32 104	2.02	3.2	.270	–
F1g22	30 852	2.34	4.5	.250	–
F1g30	31 358	1.92	4.6	.248	–
F1g31	29 984	2.33	3.6	.306	–
F1g38	31 021	2.22	3.9	.294	–
F1g43	33 099	2.29	3.1	.279	–
F1g44	30 605	–	–	–	–
F1g58	30 654	–	–	–	–
F1g65	31 049	2.18	4.0	.321	–
F1g76	30 898	2.03	6.4	.346	–
F1g77	42 272	1.66	4.6	.242	–
F1g80	32 312	2.01	3.9	.289	–
F1g88	32 122	2.03	5.4	.321	–
F2g1	30 484	1.55	4.0	.182	–
F2g1A	31 475	2.02	4.1	.264	–
F2g3	31 605	1.93	4.4	.244	–
F2g5	31 100	1.95	3.8	.302	–
F2g7A	31 005	1.95	4.9	.306	–
F2g7B	30 510	1.78	3.3	.281	–
F2g9	30 151	2.02	5.1	.301	–
F3g1	17 871	1.93	4.1	.332	–
F3g2	30 169	1.86	4.1	.296	–
F3g3	31 164	1.86	4.8	.280	–
F3g4	10 988	–	–	–	–
F3g5	30 343	1.45	3.8	.220	–
F3g7	31 284	1.95	3.5	.324	–
F10g5	35 868	1.92	3.2	.268	–
F10g6	31 037	1.97	3.9	.274	–
F10g7	30 370	1.78	5.1	.237	–
F10g8	32 834	1.86	3.9	.264	–
F10g9	31 094	1.63	3.6	.224	–
Abell 119					
D26	13 462	1.90	4.0	.263	2.238
D36	13 958	1.96	3.8	.317	–
D37	12 872	–	5.0	.326	2.380
D38	12 591	1.91	3.6	.317	–
D41	12 342	–	4.1	.333	2.238
D44	13 081	–	3.2	.332	2.303
D45	12 660	–	–	–	–
D47	14 628	1.30	3.0	.278	2.288
D49	13 733	1.65	2.7	.250	2.464
D51	12 540	1.99	5.3	.321	–
D52	13 447	1.84	4.6	.348	2.422
D60	11 565	–	4.3	.319	2.520
D62	13 077	–	3.6	.338	2.207
D66	13 356	–	5.0	.334	2.431
D68	12 225	–	4.6	.325	2.342
D74	12 647	–	3.7	.257	2.396
D75	11 560	–	2.9	.273	2.223
D93	11 705	–	4.7	.289	2.322
D94	12 553	2.06	4.1	.312	–
D99	13 540	–	3.0	.305	2.428
D102	13 258	2.03	5.0	.195	2.292
D105	13 350	1.70	3.9	.303	2.496
D107	13 085	1.03	3.6	.333	2.196

Table 6. continued.

Galaxy	cz	D4000	NaD	Mg_2	$\log\sigma$
D109	13 021	–	3.5	.212	2.350
D111	12 585	1.58	4.4	.272	2.396
D112	14 650	1.46	2.8	.244	2.340
D114	13 375	2.03	4.1	.336	2.107
Abel 3125					
D9	18 508	1.50	–	.295	–
D11	8682	–	–	–	–
D14	15 532	–	–	–	–
D46	17 830	1.69	4.7	.299	2.403
D47	17 745	1.81	4.1	.292	2.476
D48	17 346	2.19	3.3	.223	–
D51	18 845	2.13	4.6	.323	2.328
D60	17 478	1.59	3.9	.304	2.464
D77	17 298	–	–	–	2.417
D88	17 693	1.11	5.0	.333	2.521
D93	17 621	1.27	3.2	.294	2.458
D95	17 866	–	–	.287	2.525
D96	17 652	2.38	2.3	.238	2.378
D103	17 766	1.59	3.3	.208	2.459
D104	18 099	1.72	3.1	.271	–
D129	18 890	1.52	2.9	.265	–
D130	19 049	1.58	3.5	.294	2.373
D140	18 945	1.69	4.2	.232	2.326
D160	18 459	1.44	3.5	.297	2.418
D161	17 964	1.73	3.1	.358	2.516
Abel 3330					
g1	27 522	1.63	4.5	.285	–
g2	26 446	1.09	2.1	.267	–
g3	27 358	2.75	3.7	.301	–
g4	26 586	2.06	–	.283	–
g5	28 262	1.54	6.0	.355	–
g6	27 140	1.77	4.3	.299	–
g7	26 222	–	–	–	–
g21	26 463	1.59	3.4	.365	–
g22	28 251	1.53	3.5	.288	–
Abell 1069					
D3	19 336	1.22	5.1	.267	–
D9	19 478	2.50	3.9	.269	–
D12	16 624	1.72	2.6	.288	–
D14	16 656	1.44	3.9	.310	–
D15	19 709	1.57	4.2	.317	2.378
D16	20 110	1.06	5.5	.175	–
D19	18 040	1.16	4.0	.285	2.342
D21	193 45	1.26	3.5	.352	2.553
D25	20 247	1.88	2.6	.243	2,439
D29	20 067	2.06	4.8	.307	2.373
D30	20 430	1.28	3.7	.254	–
D38	19 432	–	–	.279	2.470
D39	19 729	–	2.0	.227	–
D41	11 644	–	–	–	–
D46	19 653	2.03	5.1	.331	2.364
D47	18 931	–	–	.274	2.173
Abell 1983					
D6	17 547	1.69	2.2	.214	–
D10	13 156	1.63	5.5	.331	–
D15	13 676	2.14	4.5	.340	2.509

Table 6. continued.

Galaxy	cz	D4000	NaD	Mg_2	$\log\sigma$
D23	12 782	1.49	2.5	.182	–
D24	13 504	1.62	4.6	.269	–
D26	17 822	1.93	4.6	.322	–
D28	6251	1.60	2.1	.205	–
D35	13 659	2.39	4.3	.265	–
D46	13 532	2.18	2.9	.308	–
D54	12 979	1.82	4.9	.315	2.365
D56	13 583	2.07	5.0	.282	2.297
D58	13 606	2.06	2.8	.240	–
D77	13 844	–	–	.283	2.332
D78	13 639	1.88	4.1	.294	2.326
D84	13 894	1.99	5.0	.309	–
D105	13 387	2.01	4.5	.340	2.509
Abel 2151					
D4	9986	1.92	2.9	.264	–
D7	10 055	2.24	4.2	.335	–
D9	10 248	1.91	2.7	.306	–
D15	9966	1.97	3.6	.326	–
D40	10 050	2.13	4.1	.285	2.362
D62	9338	2.37	4.2	.278	–
D63	10 455	2.44	4.1	.276	2.290
D64	10 432	1.98	6.0	–	–
D65	10 426	–	–	.319	2.464
D66	9643	–	–	.284	2.270
D78	10 262	–	–	–	–
D134	11 074	–	–	.316	2.502
DC2103-39					
D3	16 152	1.37	4.5	.294	2.267
D14	9343	1.31	5.0	.342	2.521
D15	15 038	1.36	3.5	.338	2.375
D18	9208	–	–	–	2.137
D20	9353	1.01	1.9	.206	2.188
D21	9400	1.50	2.6	.233	2.384
D23	9245	1.26	2.7	.259	2.415
D38	15 742	1.64	3.3	.234	2.439
D39	15 892	1.23	1.3	.290	2.496
D40	14 992	1.51	4.2	.282	2.348
D42	14 700	1.51	3.9	.271	2.314
D53	26 558	2.06	4.3	.348	2.500
D60	15 626	1.29	4.0	.254	2.248
D61	15 326	1.37	3.4	.311	2.301
D62	15 079	1.11	1.7	.252	2.246
D63	14 937	1.20	2.2	.293	2.167
D66	9581	1.19	–	.192	2.371
D71	14 832	1.41	4.4	.280	2.316
D73	14 940	–	–	.298	2.415
D76	15 230	1.70	4.3	.220	–
D102	15 324	–	–	–	2.316